e-Polymers **2009**, no. 049

http://www.e-polymers.org

ISSN 1618-7229

Influence of the lignin on thermal degradation and melting behaviour of poly(ethylene terephthalate) based composites

Maurizio Canetti,* *Fabio Bertini*

*Istituto per lo Studio delle Macromolecole - C.N.R. Via Bassini 15-20133 Milano (Italy); fax +390270636400; e-mail: canetti@ismac.cnr.it

(Received: 22 December, 2007; published: 28 May, 2009)

Abstract: Poly(ethylene terephthalate) (PET) has been compounded with lignin (L) by a single-screw extruder. The influence of L presence and its content on the thermal stability of PET has been studied by using thermogravimetric analysis. The experiments carried out in oxidative conditions evidenced the barrier effect of L that interferes to the diffusion of the volatile degradation products to the gas phase and at the same time to the diffusion of the oxygen from the gas phase to the PET matrix. The influence of L on the melting behaviour of PET has been investigated on samples submitted to subsequent annealing steps procedure. X-ray techniques were employed to investigate crystallinity and crystal dimensions of pure PET and PET/L composites. Considering the supermolecular and crystal structure of the annealed samples, their melting behaviour was explained assuming small changes in the melting entropy.

Introduction

Lignin (L), a natural polyphenolic plant constituent, is easily available and relatively inexpensive. L structure and properties depend on wood species and processing condition, but standard well-defined L was obtained as a byproduct of industrial papermaking [1]. When heated at high temperature, L is able to give a large amount of char; this feature is a basic aspect of flame retardant additives, since char reduces the conbustion rate of polymeric materials [2]. The antioxidant properties of L were used to stabilize polymer matrix composites against photo- and thermo-oxidation [3-5]. The intermolecular interactions occurring in blends based on L and synthetic polymers were also investigated [6-8]. Previous papers reported about the nucleation effect of L during the crystallization of the polymeric matrix [9-11].

Poly(ethylene terephthalate) (PET) is a thermoplastic polymer, its structure and physical properties have been extensively studied. Opposite interpretations have been reported about PET structural organization and thermal behaviour [12-22].

PET has been blended or compounded with several polymers or nanofillers, with the aim to change its physical and mechanical properties [23-26]. Morphological analysys of PET/L composites evidenced that L particles were well dispersed in the PET matrix, with a diameter ranging from some tens of nm to some μm [10].

In this paper, the effect of L presence and content on thermal degradation behaviour was investigated carrying out thermogravimetric analysis (TGA) in inert and oxidative atmosphere. The influence of L particles on melting behaviour and on supermolecular parameters of PET annealed composites was studied by means of

differential scanning calorimetry (DSC), small-angle X-ray scattering (SAXS) and wide-angle X-ray diffraction (WAXD).

Results and discussion

The effect of the L presence on the thermal stability of the composites was studied by means of thermogravimetric experiments carried out in both inert and oxidative conditions. The TGA and derivative thermogravimetry (DTG) experimental data, i.e. the temperature corresponding to initial 5% of weight loss (T_5), the temperature of maximum rate of weight loss (T_{mr}) and the char yield obtained at different temperatures, are reported in Tab. 1 for the runs carried out at 10 °C·min^{-1}. The residue amount was calculated at 600 °C, corresponding to the final temperature of degradation for the experiments conducted in nitrogen, while for the ones carried out in air, the residue value was calculated at the end of the first step of the oxidative degradation (about 485 °C), i.e. before the char oxidation step.

Tab. 1. TGA data under nitrogen and air atmosphere for pure PET and PET/L composites.

Sample	Atmosphere	T_5 (°C)	T_{mr} (°C)	Residue (wt%)
PET	N_2	403	438	14.8
PET/L 97.5/2.5	N_2	397	438	15.4
PET/L 95/5	N_2	396	439	15.9
PET/L 90/10	N_2	385	439	16.8
PET/L 80/20	N_2	365	436	19.5
PET	Air	396	434	17.9
PET/L 97.5/2.5	Air	396	438	18.5
PET/L 95/5	Air	394	440	19.4
PET/L 90/10	Air	384	437	22.1
PET/L 80/20	Air	365	431	26.7

The TGA and DTG curves, obtained under nitrogen atmosphere, of pure PET, pure L and some selected PET/L composites are shown in Fig. 1. The pure PET volatilizes in a single step, from 300 to 500 °C. The thermal behaviour of L is completely different. Above 200 °C the lignin shows a slow weight loss with a characteristic T_{mr} of 368 °C. The thermal decomposition of L in inert atmosphere produce a remarkable char residue, higher than 35 wt.% at 700 °C. In general, if compared to the pure PET the composites show a decrease of thermal stability in nitrogen. The initial temperature of degradation decreases with the increase of the amount of L in the composites, whereas the T_{mr} is quite constant (436-439 °C) for all the investigated samples. The char yield for the composites increases as a function of the L amount.

Fig. 2 reports the TGA curves, obtained under air atmosphere, of pure PET, pure L and some composites. The TGA thermograms of PET and composites almost superimpose on those obtained under inert atmosphere up to 450 °C; the oxidative atmosphere seems to have little effect on the thermal degradation process of the PET and of the composites in the initial temperature range. Above 450 °C, however, the degradation of pure PET carried in air atmosphere is characterized by a remarkable weight loss with a maximum at around 560 °C. This degradation stage is due to the oxidation process of the char residue. The L thermogram shows a broad degradation region between 200 and 500 °C, associated with the evolution of organic

products. The corresponding DTG curve (not shown) is characterized by various overlapping peaks due to the different mechanisms involved in the evolution of the decomposition products. The L is completely degraded at 510 °C.

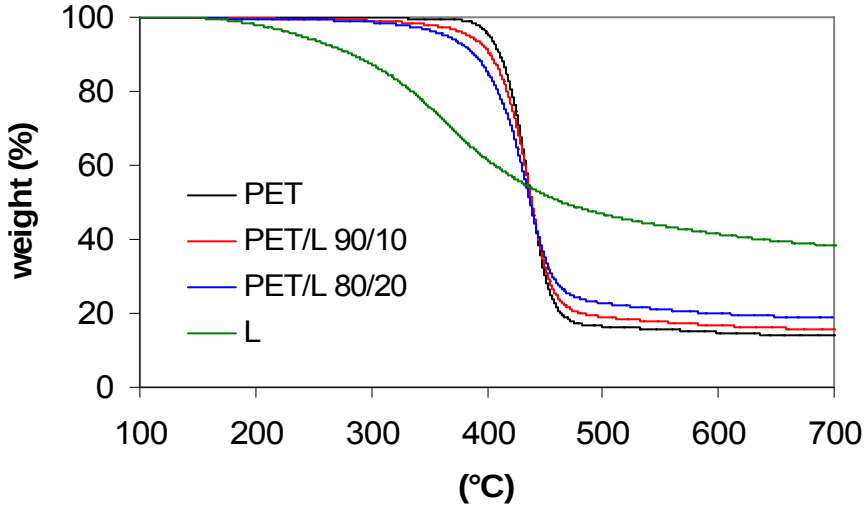

Fig. 1. TGA thermograms under inert atmosphere.

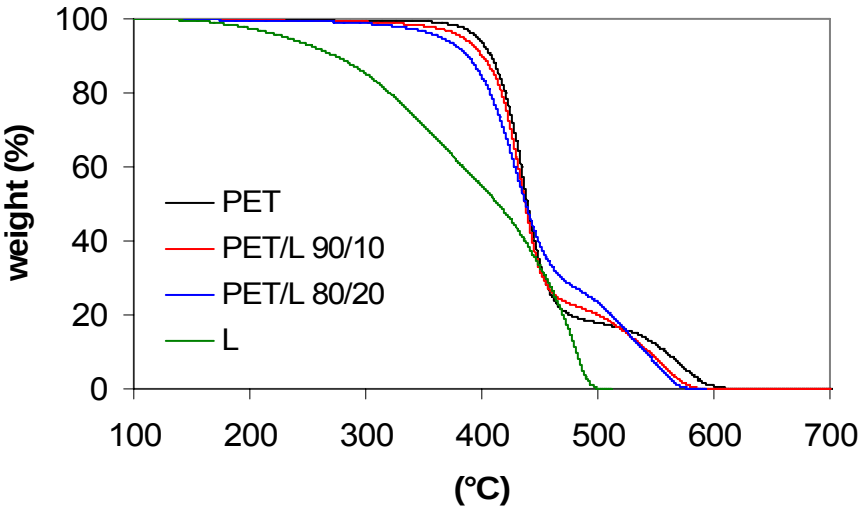

Fig. 2. TGA thermograms under oxidative atmosphere.

It is observed that in the composites the initial weight loss takes place at lower temperature than that for pure PET and the T_5 value progressively decreases with increasing the L content in the composite. As shown in Tab. 1, the characteristic T_{mr} values for the composites are similar, ranging from 431 to 440 °C, and close to that of the pure PET. In the temperature range between the T_{mr} values and about 520 °C, the weight loss for the composites decreases as a function of L content. This unexpected behaviour could be due to the interactions occurring by blending the polyester and the L. In order to investigate deeply the thermal behaviour of the composites, theoretical TGA curves in inert and oxidative atmosphere were calculated for PET/L 80/20 sample from individual weight loss data of pure

components, recorded at 20 °C·min^{-1}. To emphasize the synergistic effect obtained by blending the components, the theoretical TGA curves were compared with the experimental ones as shown in Fig. 3.

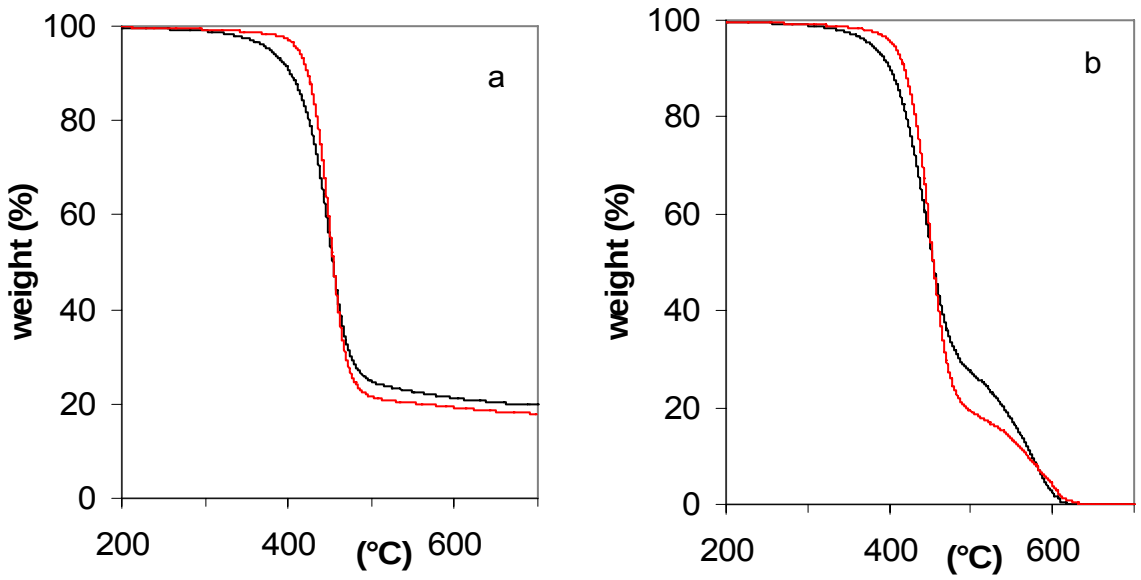

Fig. 3. TGA for PET/L 80/20 under inert (a) and oxidative (b) atmosphere at 20 °C·min^{-1}: (—) experimental thermogram, (—) theoretical thermogram calculated from individual weight loss data of pure components.

Marked differences between theoretical and experimental curves are observed in both adopted atmospheres. In general, in the temperature range 300-460 °C the experimental thermograms are shifted toward lower temperatures, while an opposite behaviour is observed at higher temperatures.

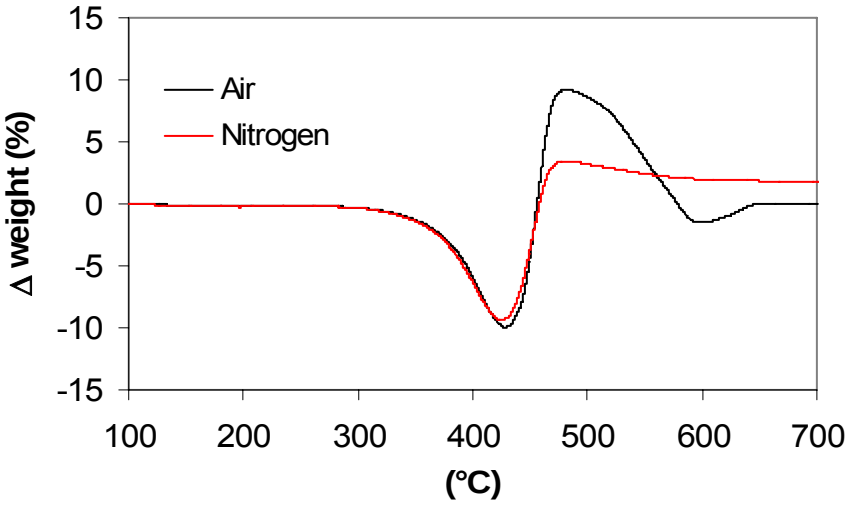

Fig. 4. Δweight (%) vs. temperature curves for PET/L 80/20 composite in inert and oxidative atmosphere.

To point out the interactions occurring between the composite components during the thermal degradation process, the Δweight values (ΔW) were calculated by subtracting the theoretical curves from the experimental ones, as a function of temperature. The profiles reported in Fig. 4 show that the ΔW values calculated in both inert and oxidative atmosphere are quite the same up to 460 °C. In the temperature range 460-565 °C, the enhancement of the ΔW values is much higher for the degradation performed in air atmosphere. The improvement in the thermal stability is due to a physical barrier effect of the char yield; in fact, the char is a carbon-based residue that undergoes slow oxidative degradation. The barrier effect concerns the diffusion of the volatile thermal oxidation products to the gas phase and, at the same time, of the oxygen from the gas phase to the PET matrix.

In this section we focus our attention on melting behaviour and structural properties of pure PET and PET/L 80/20 composite. PET exhibits multiple melting endotherms depending on its thermal history, as revealed by DSC investigation [16, 17, 19, 21]. DSC scans of pure PET isothermally crystallized at 230 °C for 35 min, and of PET/L 80/20 composite isothermally crystallized at 230 °C for 20 min, as reported in Fig. 5 (run a) and Fig. 6 (run a), respectively. Both samples show a broad endothermic profile due to the melting of the crystals formed during the primary crystallization and to the fusion of the crystals obtained as a result of recrystallization on heating. If compared to those of pure PET, the melting endotherms in PET/L is more separated and, at lower temperature, centred.

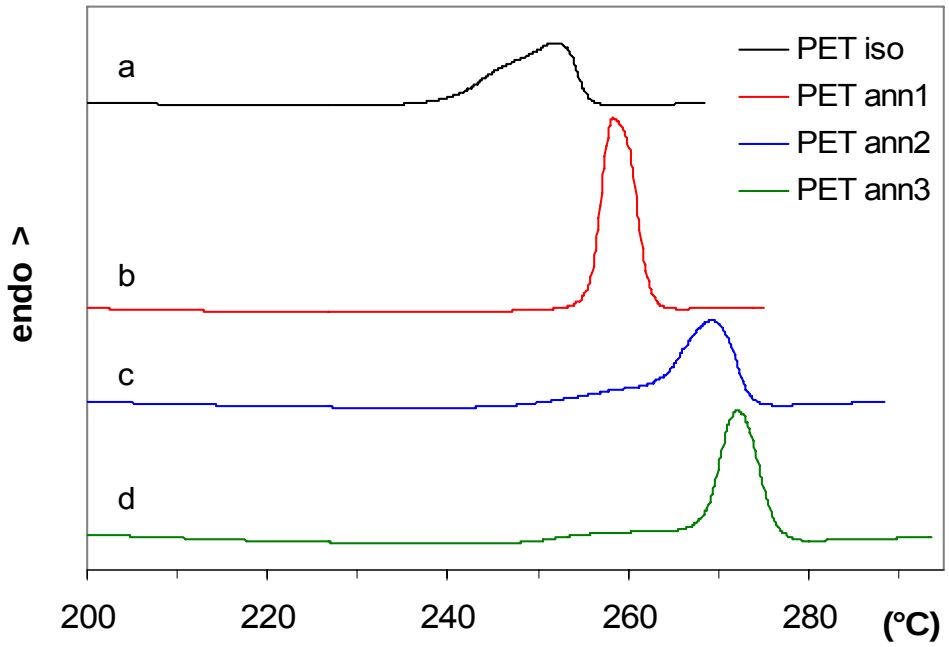

Fig. 5. DSC scans of pure PET.

The isothermally crystallized samples were submitted to three subsequent annealing steps carried out at 230 °C for 15 h (ann1), at 245 °C for 16 h (ann2), and at 245 °C for 64 h (ann3). At the end of every single annealing step the samples were examined by DSC and X-ray techniques. DSC melting traces of pure PET and of PET/L 80/20 composite annealed samples are reported in Fig. 5 and Fig. 6, respectively.

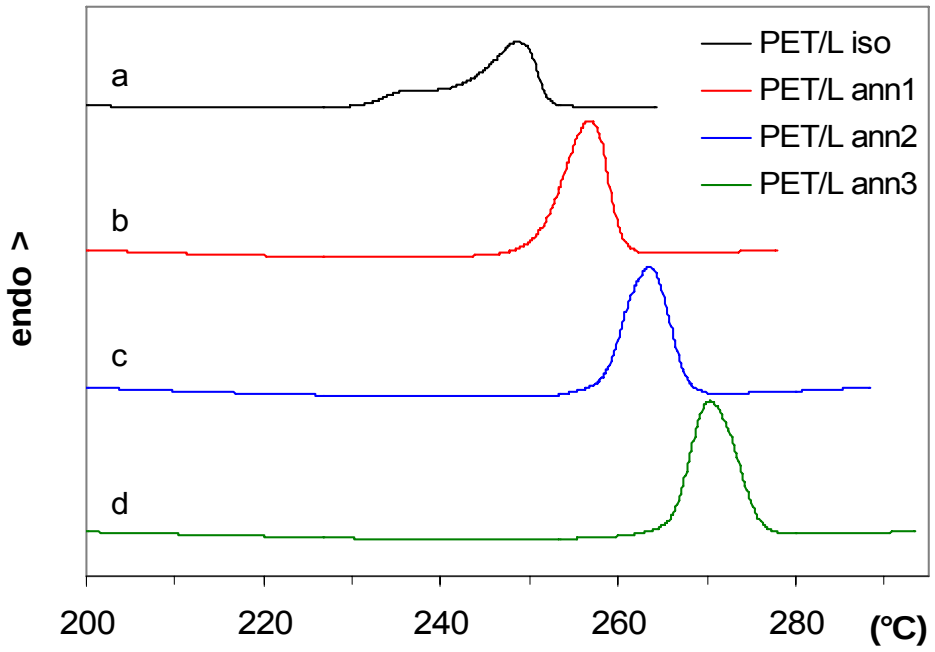

Fig. 6. DSC scans of PET/L 80/20.

It can be observed that after the first annealing step both samples exhibit a single endothermic event. The position of the melting peak moves to a higher temperature and the enthalpy of fusion is increased (Fig. 5 run b, and Fig. 6 run b).

The successive annealing steps induce the progressive enhancement of the melting temperature (T_m), whereas the enthalpy of fusion involved remains quite constant, for pure PET and PET/L 80/20 composite samples (Fig. 5 runs c-d, and Fig. 6 runs c-d). Narrow melting peaks are registered for the PET/L 80/20 composite, while the melting peaks of the pure PET are preceded by a broad endothermic event. These different behaviour can be ascribed to the fact that the adopted annealing times are not enough to allow a complete reorganization of the crystalline structure for the pure PET. Instead, the presence of L in the composite promotes the crystallization process and induces the complete crystalline reorganization [10].

It is interesting to point out that the T_m values of the pure PET are higher than those of the PET/L 80/20 composite, for all the adopted thermal treatments.

The aforementioned melting behaviour of the pure PET and PET/L 80/20 composite could be an indication of a significant evolution of the supermolecular structure mainly in terms of the PET crystal dimensions. All the isothermally crystallized and annealed samples were submitted to SAXS and WAXD characterization.

The SAXS data were analyzed using the pseudo-two-phase model [27, 28]. The long period (L_p), the thickness of the transition layer (E), the phase thicknesses, $\langle T_1 \rangle_n$ and $\langle T_2 \rangle_n$, and the linear fraction of the phases , X_1 and X_2, respectively, are reported in Tab. 2. SAXS investigation unambiguously provides the value of the L_p, while, the phase thicknesses $\langle T_1 \rangle_n$ and $\langle T_2 \rangle_n$ can be assigned to the crystalline and amorphous region or vice versa, according to the Babinet's reciprocity theorem. This ambiguity determined opposite interpretation on the SAXS data for PET [17, 22]. Considering

the results obtained by WAXD reported in Tab. 3, we are inclined to assign the smaller values $\langle T_1 \rangle_n$ and X_1 to the crystalline phase.

Tab. 2. Supermolecular parameters calculated by SAXS.

Sample	L_p (nm)	$\langle T_1 \rangle_n$ (nm)	$\langle T_2 \rangle_n$ (nm)	E (nm)	X_1	X_2
PET iso	12.8	4.6	8.2	1.4	0.36	0.64
PET ann1	12.7	4.9	7.8	1.2	0.39	0.61
PET ann2	12.7	5.2	7.5	1.3	0.41	0.59
PET ann3	12.7	5.0	7.7	1.2	0.39	0.61
PET/L 80/20 iso	12.6	4.8	7.8	1.3	0.38	0.62
PET/L 80/20 ann1	12.7	5.0	7.7	1.3	0.39	0.61
PET/L 80/20 ann2	12.8	5.0	7.8	1.1	0.39	0.61
PET/L 80/20 ann3	12.8	4.8	8.0	1.1	0.38	0.62

As a function of the annealing treatment the supermolecular parameters reported in Tab. 2, show small dimensional differences. Such differences do not justify the melting behaviors in terms of T_m values, shown in Figs. 5 and 6. The trend of the $\langle T_1 \rangle_n$ value as a function of the annealing steps seems to exclude the lamellae thickening for the PET/L 80/20 composite. For the pure PET a small increase of the $\langle T_1 \rangle_n$ value is evidenced as a function of annealing treatment. The soundness of these findings has to be pointed out because of the attribution of $\langle T_2 \rangle_n$ as crystalline thickness draws to the same conclusions, i.e. the absence of marked thickening phenomena.

Tab. 3. Crystallinity and crystal dimension determined by WAXD.

Sample	X_c	$X_{c\,PET}$	$D_{0\text{-}11}$ (nm)	D_{010} (nm)	D_{100} (nm)
PET iso	0.29	0.29	11.5	10.9	9.4
PET ann1	0.32	0.32	13.2	14.5	10.7
PET ann2	0.33	0.33	14.8	15.9	10.8
PET ann3	0.35	0.35	15.1	15.2	10.4
PET/L 80/20 iso	0.27	0.34	13.3	13.5	9.0
PET/L 80/20 ann1	0.29	0.36	13.6	13.5	10.1
PET/L 80/20 ann2	0.30	0.37	13.5	13.9	10.7
PET/L 80/20 ann3	0.30	0.37	15.3	14.6	10.4

The supermolecular parameters calculated for pure PET and PET/L 80/20 samples are similar, thus they suggest the absence of L particles in the interlamellar region of PET. As reported in our previous paper [10], the L particles mainly relegate to the intraspherulitic regions of PET.

In Tab. 3 the bulk crystallinity, X_c, the crystallinity of the PET component, $X_{c\,PET}$, and crystal dimension D_{hkl}, determined by WAXD analysis are reported. In general, the annealing treatments produce a small increase in bulk crystallinity for pure PET and PET/L 80/20 composite (Fig. 7); the lateral crystal dimensions, developed in the normal direction with respect to the lamellar thickness (D_{010} and D_{100}), increase going on from the isothermally crystallized sample to the annealed ones. However, the successive annealing steps do not induce a progressive increase of the D_{hkl} values.

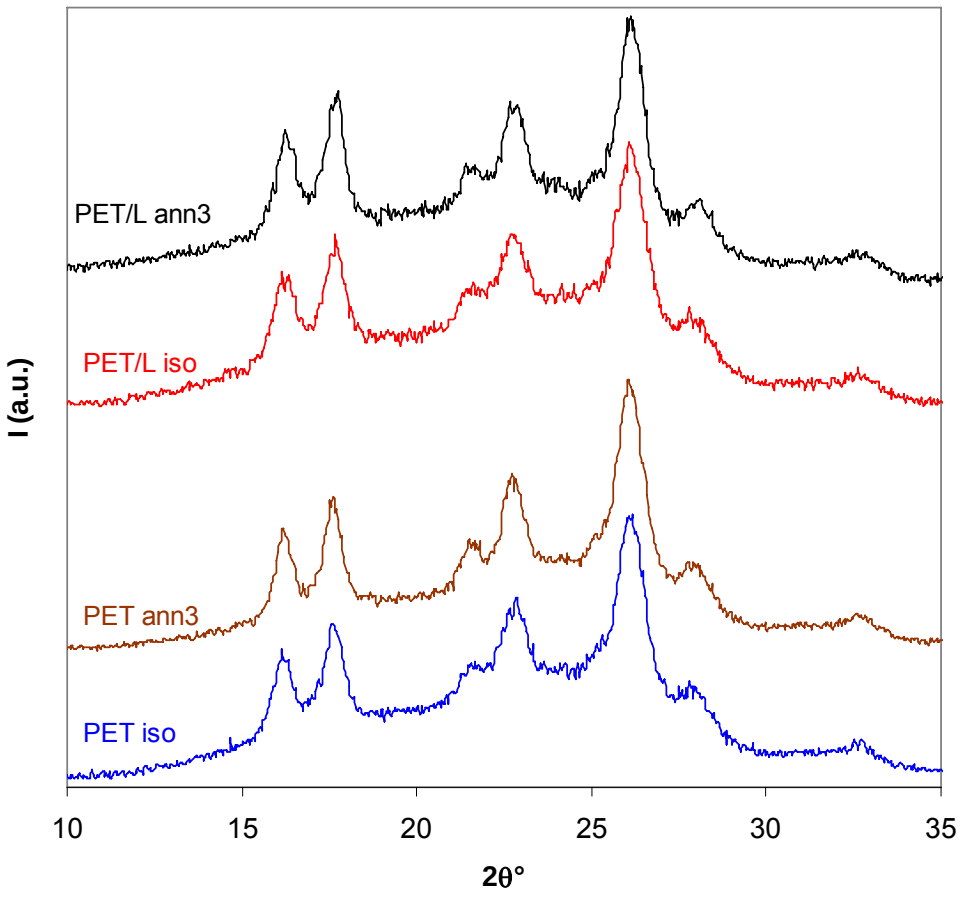

Fig. 7. WAXD diffractograms of PET and PET/L 80/20.

In conclusion, for pure PET and PET/L 80/20 composite samples, a progressive enhancement in the melting temperature was observed as a function of the annealing treatment. Nevertheless, such trend was not accompanied by a significant increase in the thickness or lateral dimensions of the PET crystal. Wang et al. [17] attributed the increase of the T_m value to transesterification phenomena occurring in the amorphous phase of the PET, in accordance with the explanation given earlier by Wunderlich [29]. The change in the conformation of the amorphous chains between lamellae reduces the entropy of melting, and determines an increase of melting temperature.

Conclusions

In this paper PET has been compounded with different amount of L by a single-screw extruder. The influence of the L presence and its content on thermal degradation behaviour has been investigated. For the PET based composites it is observed that the initial weight loss occurs at lower temperature than that of pure polyester; the temperature corresponding to the max rate of weight loss being close to that of pure PET does not depend on the L content. The experiments carried out in air atmosphere evidence that the presence of L in the composites favours the formation of a protective surface shield able to reduce the oxygen diffusion towards the polymer bulk. The L presence strongly influences the melting behaviour of annealed samples. In particular, L presence in the composite promotes the crystallization

process and induces a faster crystalline reorganization than that of the pure PET. The trend of the T_m values as a function of the annealing treatment cannot be justified by the calculated supermolecular and crystal parameters for both pure PET and PET/L composite. The reduction in the entropy of melting due to a modification of the amorphous phase has to be considered as responsible of the melting behaviour.

Experimental part

PET (Caripack P82, Shell), and hydrolytic lignin, L (Aldrich, CAS n. 8072-93-3) were used in preparing composites with PET/L weight ratios 100/0, 97.5/2.5, 95/5, 90/10 and 80/20. The composites were prepared by mechanical mixing followed by thermal extrusion using a Brabender Plasticorder PLV 151 with Extrusiongraph 25D single screw extruder, extrusion temperatures: 250/255/260/225 °C. On processing, dry nitrogen was continuously purged into the chamber to ensure minimum thermo-oxidative degradation.

Thermogravimetric analysis (TGA) was carried out with a Perkin-Elmer TGA 7 instrument. The sample (ca. 3 mg) was heated from 50 to 700 °C at different heating rates (10 and 20 °C·min^{-1}) under a nitrogen or air atmosphere (60 mL·min^{-1}).

Differential scanning calorimetry (DSC) scans were carried out on a Perkin-Elmer Pyris 1 instrument under nitrogen atmosphere. The sample was heated with a scan rate of 20 °C·min^{-1} from 50 to 290 °C determining the melting temperature and the enthalpy of fusion.

Small-angle X-ray scattering (SAXS) measurements were conducted at 22 °C with a Kratky Compact Camera. Monochromatized Cu K_α radiation (λ = 0.154 nm) was supplied by a stabilized Siemens Krystalloflex 710 generator and a Siemens FK 60-04, 1500W Cu target tube operated at 40 kV and 30 mA. The scattered intensity was counted in different ranges of 2θ°, by using a step scanning proportional counter with pulse height discrimination.

Wide angle X-ray diffraction (WAXD) data were obtained at 20 °C using a Siemens D-500 diffractometer equipped with a Siemens FK 60-10 2000W tube (Cu K_α radiation, λ = 0.154 nm). The operating voltage and current were 40 kV and 40 mA, respectively. The data were collected from 5 to 40 2θ° at 0.02 2θ° intervals.

References

[1] Glasser, W.G.; Sarkanen, S. *Lignin: properties and materials*, **1989**, American Chemical Society, Washington.
[2] Canetti, M.; Bertini, F.; De Chirico, A.; Audisio, G. *Polym. Degrad. Stab.* **2006**, *91*, 494.
[3] Alexy, P.; Kosikova, B.; Podstranska, G. *Polymer* **2000**, *41,* 4901.
[4] Pouteau, C.; Dole, P.; Cathala, B.; Averous, L.; Boquillon, N. *Polym. Degrad. Stab.* **2003***, 81*, 9.
[5] Gregorova, A.; Kosikova, B.; Stasko, A. *J. Appl. Polym. Sci.* **2007**, *106*, 1626.
[6] Kadla, J.F.; Kubo, S. *Macromolecules* **2003**, *36*, 7803.
[7] Kadla, J.F.; Kubo, S. *Compos. Part A* **2004**, *35*, 395.
[8] Kubo, S.; Kadla, J.F. *J. Appl. Polym. Sci.* **2005**, *98*, 1437.
[9] Canetti, M.; De Chirico, A.; Audisio, G. *J. Appl. Polym. Sci.* **2004**, *91*, 1435.
[10] Canetti, M.; Bertini, F. *Comp. Sci. Technol.* **2007,** *67*, 3151.
[11] Weihua, K.; He, Y.; Asakawa, N.; Inoue, Y. *J. Appl. Polym. Sci.* **2004**, *94*, 2466.

[12] Santa Cruz, C.; Stribeck, N.; Zachmann, H.G.; Balta Calleja, F.J. *Macromolecules* **1991**, *24*, 5980.
[13] Goshel, U.; Urban, G. *Polymer* **1995**, *19*, 3633.
[14] Medellin-Rodriguez, F.J.; Phillips, P.J.; Lin, J.S. *Macromolecules* **1996**, *29*, 7491.
[15] Verma, R.K.; Hsiao, B.S. *Trends Polym. Sci.* **1996**, *4*, 312.
[16] Medellin-Rodriguez, F.J.; Phillips, P.J.; Lin, J.S.; Campos, R*. J. Polym. Sci. B: Polym. Phys.* **1997,** *35,* 1757.
[17] Wang, Z.G.; Hsiao, B.S.; Sauer, B.B.; Kampert, W.G. *Polymer* **1999**, *40*, 4615.
[18] Wang, Z.G.; Hsiao, B.S.; Fu, B.X.; Liu, L.; Yeh, F.; Sauer, B.B.; Chang, H.; Schultz, J.M. *Polymer* **2000**, *41*, 1791.
[19] Lu, X.F.; Hay, J.N. *Polymer* **2001**, *42*, 9423.
[20] Ivanov, D.A.; Amalou, Z.; Magonov, S.N. *Macromolecules* **2001**, *34*, 8944.
[21] Kong, Y.; Hay, J.N.; *Polymer* **2003**, *44*, 623.
[22] Haubruge, H. G.; Jonas, A.M.; Legras, R. *Macromolecules* **2004**, *37*, 126.
[23] Galeski, A. *e-Polymers* **2002**, no. 026.
[24] Li, Z.; Luo, G.; Wei, F.; Huang, Y. *Comp. Sci. Tech.* **2006**, *66*, 1022.
[25] Fan, X.; Chen, D. *e-Polymers* **2007**, no. 116.
[26] Jin, S.H.; Park, Y.B.; Yoon, K.H. *Comp. Sci. Tech.* **2007**, *67*, 3434.
[27] Strobl, G. R.; Schneider, M. *J. Polym. Sci. Polym. Phys. Ed.* **1980,** *18*, 1343.
[28] Vonk, C. G. *J. Appl. Cryst.* **1973**, *6*, 81.
[29] Wunderlich, B.; *Macromolecular physics,* **1976**, vol. 2, Academic Press, New York.